RESEARCH ARTICLE

Development of Novel Nanofiber Patches Loaded with *Boerhavia diffusa* Root Phytochemicals for Enhanced Wound Healing: A Response Surface Methodology Approach

Smita Borkar[1], Prashant Kumar Dhakad[1], Hemant Kumar Singh Yadav[2]

[1]*School of Pharmacy, Suresh Gyanvihar University, Jaipur, Rajasthan, India*
[2]*Department of Pharmaceutical Sciences, Indira Gandhi University, Meerpur, Rewari, India*

Received: 6th Apr, 2025; Revised: 20th May, 2025; Accepted: 10th Jun, 2025; Available Online: 25th Jun, 2025

ABSTRACT

This research focuses on the development and optimization of a novel nanofiber patch loaded with *Boerhavia diffusa* root extract for enhanced wound healing by Response Surface Methodology (RSM) method. *Boerhavia diffusa*, a traditional medicinal plant, is known for its wound healing properties through stimulation of angiogenesis, collagen formation, and epithelialization. The methanolic extract was incorporated into polyvinyl alcohol (PVA) and polyethylene oxide (PEO) solutions at 8 mg/mL concentrations and electrospun into nanofiber mats under optimized conditions.

The study employed a 3^2 factorial design using RSM with Design Expert-7 for evaluating drug entrapment efficiency and swelling index. Characterization techniques were applied to analyze nanofiber's morphology, structural properties, thermal behavior, and crystallinity. The optimized batch (BDRNF7) demonstrated 85.12% drug entrapment efficiency, uniform thickness, and sustained drug release. Additionally, chitosan/alginate membrane dressings were synthesized through physical blending and covalent crosslinking to evaluate film uniformity, mass, pH, and drug content. BDRNF7 showed significant wound contraction, enhanced skin breaking strength, and effective wound healing compared to controls. Moisture interaction studies indicated the patch's stability under varying humidity. Statistical analysis confirmed the model's significance (F-value: 11.88, Adjusted R^2: 0.8718). In conclusion, the developed nanofiber patch exhibited potential as a bioactive wound dressing, providing effective drug delivery and accelerated wound healing. Further studies will validate its clinical application in wound care management.

Keywords: Crosslinking, Clinical application, Wound contraction, Response Surface Methodology

How to cite this article: Smita Borkar, Prashant Kumar Dhakad, Hemant Kumar Singh Yadav. Development of Novel Nanofiber Patches Loaded with *Boerhavia diffusa* Root Phytochemicals for Enhanced Wound Healing: A Response Surface Methodology Approach. International Journal of Drug Delivery Technology. 2025;15(2):796-803. doi: 10.25258/ijddt.15.2.55

Source of support: Nil.

Conflict of interest: None

INTRODUCTION

Any disruption to the skin's natural continuity is called a wound. Overall, there are four distinct phases to wound healing: haemostasis, inflammation, proliferation, and maturation[1]. Repairing damaged tissues and re-establishing their normal function depends on the intricate biological process known as wound healing[2]. Chronic wounds, infections, and diminished quality of life are all possible outcomes of impaired wound healing[3,4]. General investigation has been carried out over years to create novel approaches and materials that can improve healing process of wounds[5,6]. Wound dressings made of nanofiber are one option; these have many benefits, like great mechanical qualities, & capability to contain bioactive substances for controlled and prolonged release[7,8]. This article delves into the topic of nanofiber manufacture using 3^2-factorial design Response Surface Methodology (RSM). The nanofiber will contain extract from *Boerhavia diffusa*, a traditional medicinal plant known for its established wound healing qualities."Punarnava" or "Hogweed," the common names for the plant *Boerhavia diffusa*, have deep roots in ancient medical practices like Ayurveda and TCM. The anti-inflammatory, antioxidant, antibacterial, and wound healing characteristics of its several bioactive components—alkaloids, flavonoids, and saponins—have prompted substantial research into this plant[9]. *Boerhavia diffusa* extract has shown promise as a wound healing agent because to its ability to stimulate angiogenesis, collagen formation, and epithelialisation, as demonstrated in many investigations[10]. The distinctive structural and functional properties of nanofiber-based wound dressings have recently attracted a great deal of interest[11]. Fabricated utilising electrospinning processes, these materials provide a perfect habitat for cells that aid in wound healing by mimicking the natural extracellular matrix[12]. Chronic wounds, burns, and surgical incisions are just a few of the many wound types that can benefit from nanofiber wound dressings due to their improved moisture retention, breathability, and protection from external contaminants[13]. Incorporating *Boerhavia diffusa* extract into new nanofiber wound dressings utilising Response Surface Methodology (RSM) is the goal of this study[14]. Finding the sweet spot for the electrospinning

**Author for Correspondence: smita.borkaragcop@gmail.com*

Table 1: Influence of electrospinning constraints on size of the nanofiber made from PVA and PEO

	Flow rate (mLh−1)	Size (nm)	Distance (cm)	Size(nm)	Voltage(kV)	Size(nm)
Nanofiber (PVA)	0.3	416±102	5	455±108	10	410±115
	0.5	206±112	10	312±156	20	356±123
	0.7	516±251	15	154±253	30	194±147
	0.9	605±62	20	645±45	50	173±125
Nanofiber (PEO)	0.3	212±	5	124±108	10	545±115
	0.5	172±	10	655±156	20	327±123
	0.7	450±	15	219±253	30	453±147
	0.9	371±	20	197±45	50	255±125

Table 2: Independent variables

Independent Variables					Unit	Low Actual	High Actual	Low Coded	High Coded
PVA of (A)					mg/ml	6	14	-1.000	1.000
PEO (B)					mg/ml	6	14	-1.000	1.000
Response	Name	Units	Analysis	Minimum	Maximum	Mean	Std. Dev.	C.V%	Model
Y1	DEE	%	Polynomial	73.19	85.12	80.12	1.23	1.54	Quadratic
Y2	Swelling index(SI)		Polynomial	65.14	86.6	77.20	2.61	3.38	Quadratic

Table 3: Formulae for wound dressing preparation of Optimized formulation (BRNF7)

Ingredients	Formulation code			
	F1	F2	F3	F4
Chitosan: Sod.alginate	4:1	3:1	2:1	1:1
Optimised formulation (BRNF7) (ml)	0.2	0.2	0.2	0.2

process settings and then studying the shape, mechanical characteristics, drug encapsulation effectiveness, and bioactive component sustained release of the resulting nanofiber are chief goals of study. The end goal is to generate a new kind of wound dressing that uses *Boerhavia diffusa*'s healing properties to speed up the healing process.

MATERIALS AND METHODS

The *Boerhavia* diffusa plant demonstrated in figure 1 was collected from Pune, Maharashtra and shade-dried at room temperature. Dehydrated roots and leaves were pulverized, sieved through a 120-mesh screen, and authenticated by botanist D. L. Shirodkar from the Botanical Survey of India, Pune. A herbarium specimen (Voucher No. CDP-01, Ref. No. BSI/WRC/IDEN.CER./2021/H3) was deposited on April 6, 2021.

100 gm dry course size crud drug material;pulverized with chloroform and loaded in soxhlet extraction assembly. Further extraction proceeds with first solvent chloroform. Continuous method chosen for completion of extraction step. Decolorized solvent at siphon tube indicate completion of dissolved components in respective crude drug material. Further solvent ethanol treated with same crude drug once it dried and free from previous solvent. At last refluxed same plant material with distilled water and report percent yield of extract. Above method used for both parts it result chloroform, ethanol and aqueous extract obtained. Details reported in characterization.

Boerhavia diffusa Extract Loaded Nanofiber

A methanolic root extract (0.4 mg/ml) was dissolved in a PVA and PEO solution (8 mg/ml) and stirred for 72 hours at room temperature until fully solubilized, forming a translucent, uniform solution. Electrospinning was performed using a 20 kV DC offset, 15 cm air gap, 18 ga blunted needle, and a 0.3 ml/h flow rate. A 5 ml solution was used per run, with fibers collected on a 6.5 mm diameter mandrel. The scaffolds were vacuum-dried for 3 hours to remove residual solvents before testing (Table 1 and Table 2).

Table 4: Dose and No. of animals used

Name of group	Treatment	No. of animals
Normal group	Tween 80	6
Standard	Drug	6
Dressing formulations (4)	Dressings	24

Table 5: Determination of Entrapment efficiency (%) of nanofiber BDRNF1-BDRNF9

Formulation	Entrapment efficiency (%)
BDRNF1	82.02
BDRNF2	73.19
BDRNF3	77.2
BDRNF4	84.97
BDRNF5	82.66
BDRNF6	84.52
BDRNF7	85.12
BDRNF8	68.45
BDRNF9	82.96

Optimization

After QbD, formulation design and optimization are key steps. In this study, nanosponge formulations were developed using a 3^2 factorial design with center and axial points in RSM using Design Expert-7. PVA (A) and PEO (B) concentrations served as process parameters, while Drug Entrapment Efficiency (EE%) (Y1) and Swelling Index (SI) (Y2) were the dependent variables. Formulations were prepared using levels -1 and +1 for both variables[15].

Evaluation of Nanofiber

Drug Entrapment Efficiency and Drug Loading (%)

Table 6: Response DEE

Source	Sum of Squares	df	Mean Square	F-value	p-value	
Model	274.21	5	54.84	36.24	0.0070	significant
A-PVA	30.65	1	30.65	20.25	0.0205	
B-PEO	156.67	1	156.67	103.52	0.0020	
AB	9.77	1	9.77	6.45	0.0847	
A^2	0.4110	1	0.4110	0.2716	0.6383	
B^2	76.71	1	76.71	50.69	0.0057	
Residual	4.54	3	1.51			
CorTotal	278.75	8				

Fit Statistics			
Std.Dev.	1.23	R^2	0.9837
Mean	80.12	Adjusted R^2	0.9566
C.V.%	1.54	Predicted R^2	0.8138
		Adeq Precision	17.3085

Ultracentrifugation at 10,000 rpm for 30 minutes was used to test the drug entrapment effectiveness of silver nanofiber compositions. Pellets containing silver nanofiber were redissolved in distilled water after being removed from $AgNO_3$. The ultra-violet spectrophotometer was used to examine the liquid portion of the experiment[16].

Swelling Index

Formulations were immersed directly in PBS (pH 7.4) to mimic medium conditions, in order to examine the swelling capability of the nanofiber samples.

Characterization of Optimized Batch

Using a variety of methods, the study examined electrospun nanofibers. After the gold sputter coating, the morphology and diameter were evaluated using SEM. Functional groups were detected using KBr pelletised materials by FTIR. Crystallinity was determined by XRD, while solid-state characteristics were tested by DSC. By heating samples from room temperature to 800°C under nitrogen, TGA was able to analyse their thermal stability and volatile components. The results showed that there were no significant changes. The results of these investigations illuminated the features and potential uses of the nanofibers[17].

Preliminary Formulation Development

Production of the Chitosan/Alginate Membrane Dressings

Chemists used physical mixing and solvent evaporation to create chitosan polyelectrolyte membranes that were covalently crosslinked. After dissolving 3 grammes of chitosan in 200 millilitres of 2% glacial acetic acid, a solution containing 3 weight percent chitosan was created. The molar ratios used to mix it with alginate or activated alginate were 4:1, 3:1, 2:1, and 1:1. Using 0.05 ml of HCl, the pH was brought to 5.5, and then the mixture was stirred for 30 minutes. Following this, 0.2 ml of the BRNF7 optimised formulation was applied (Table 3). Prior to vacuum drying at 40 °C for 5 hours, the mixture was cast onto a glass plate, allowed to dry at ambient temperature, and then washed with methanol four or five times. Using a micrometre, the thickness of the membrane was determined[18].

Figure 1: *Boerhavia diffusa*

Table 7: Determination of Drug loading (%) of nanofiber BDRNF1-BDRNF9

Formulation	Drug loading (%)	Swelling(%)
BDRNF1	8.5	65.14
BDRNF2	7.3	72.08
BDRNF3	7.5	75.55
BDRNF4	8.9	85.23
BDRNF5	8.0	77.91
BDRNF6	7.8	83.62
BDRNF7	9	86.6
BDRNF8	6.9	69.86
BDRNF9	7.1	78.82

Characterization of Wound Dressings Film Thickness

By setting the sample on a firm foundation and pressing the probe against it, the thickness could be measured using a gauge. Thirty readings were taken throughout the sample at 15-minute, 1-hour, 3-hour, 8-hour, and 24-hour intervals, in both dry and wet situations[19].

Film Weight and Uniformity of Mass

Film wound dressings are not specifically addressed in the European Pharmacopoeia, hence an adapted mass uniformity test (2.9.5) was employed. Twenty samples of 2.5 x 2.5 cm film were randomly sliced and weighed with a 4-decimal precision on an analytical scale (KERN 870-13, Germany). It was determined the average mass ± standard deviation and the percentage deviation. No more than two samples could deviate by more than 7.5% in accordance with pharmacopoeial limitations, and no sample could exceed twice this limit. Average results with minimum and maximum values in milligrammes and percentage of film weight were provided[20].

Surface pH

Wet the films with clean water and then assessed their surface pH using a contact pH meter (Flatrode, Hamilton, CH). We tested each sample three times and reported the average values with standard deviations[21].

Drug Content Uniformity

We checked for drug content uniformity by dissolving a 10-

Table 8: Response of swelling index

Source	Sum of Squares	df	Mean Square	F-value	p-value	
Model	404.99	5	81.00	11.88	0.0343	Significant
A-PVA	165.27	1	165.27	24.24	0.0161	
B-PEO	16.97	1	16.97	2.49	0.2128	
AB	40.90	1	40.90	6.00	0.0917	
A^2	17.39	1	17.39	2.55	0.2086	
B^2	164.47	1	164.47	24.12	0.0162	
Residual	20.45	3	6.82			
CorTotal	425.44	8				

Fit Statistics			
Std. Dev.	2.61	R^2	0.9519
Mean	77.20	Adjusted R^2	0.8718
C.V.%	3.38	Predicted R^2	0.4623
		Adeq Precision	9.8881

millimeter film in 100 millilitres of isotonic phosphate buffer (pH 6.8) and shaking it every so often for six hours. Filtered via a 0.45 mm Whatman filter paper, a 5 ml sample was diluted to 20 ml using the buffer[22].

In Vitro Drug Release

The drug's release *in vitro* was examined with a DBK Instruments Automated Transdermal Diffusion Cells Sampling System. The 1 x 1 cm samples that were loaded with drugs were placed on top of a receptor compartment that was filled with ultra-pure water, on top of a cellulose acetate membrane, at 37 °C. After a day of stirring the mixture with a magnetic bar, samples were taken. A Jasco UV-Vis spectrophotometer was used to quantify the concentration of DCF at 340 nm[23].

Wound Healing Activity

Species and Strain: Albino Rabbit

Age and Weight: Weight range: 200-240g. (12-16weeks)

Gender: Either sex

Swiss-albino rats (25-30 g) will be housed in a controlled environment (12 h light/dark cycle, 22 ± 2 °C) with free access to water and food. Anesthesia will be administered using chloral hydrate (1 mL/kg) and 1% atropine. After shaving, a 215 mm² circular wound (3.2% of body weight) will be created using sterilized scissors. Wound dressings will be applied daily until complete healing. Wound area, contraction, epithelialization period, and hydroxyproline content will be monitored (Table 4)[24,25].

RESULTS AND DISCUSSION

Characterization of Nanofiber

Drug Entrapment Efficiency

Percent entrapped drug and free drug percentage of nanofiber was determined using the UV spectrophotometric. The entrapment efficiency was found to be increased with concentration of polymer increase. Batch BDRNF4 and BDRNF57 shows higher drug entrapment efficiency which provides optimum availability of drug at site without any side effects. BDRNF7 optimized batches show 85.12% entrapment efficiency as compared to other batches (Table 5).

ANOVA for Quadratic Model Response 1: DEE

Factoring uses partial sum of squares, the third coding. With 0.70% likelihood, the Model F-value of 36.24 is significant. Model terms A, B, and B^2 are significant ($p < 0.0500$), whereas terms with $p > 0.1000$ are not. The difference between Adjusted R^2(0.9566) and Predicted R^2(0.8138) is less than 0.2, indicating acceptable alignment. Signal-to-noise ratio is assessed by Adeq Precision. Aim for a ratio above 4. Signal-to-noise ratio 17.309 is good. You can navigate the design area with this model.

$DEE = 84.55+2.26\ A+5.11B-1.56AB-0.4533-6.19B^2$

The coded equation predicts responses using factor levels, with high levels as +1 and low as -1, helping compare factor impacts via coefficients (Table 6). The actual factors equation also predicts responses using original units but isn't suitable for comparing factor impacts due to scaled coefficients and a non-centered intercept (Figure 2).

Drug Loading and Swelling of Nanofiber

The optimized batch BDRNF7 with 9% drug loading provide valuable information for potential drug delivery

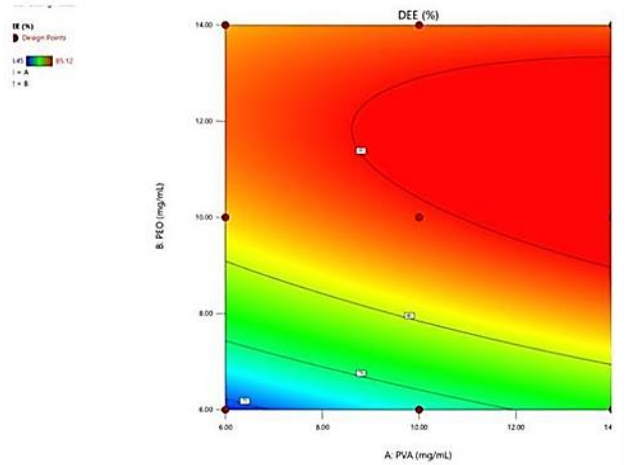

Figure 2: Counter plot of drug entrapment efficiency

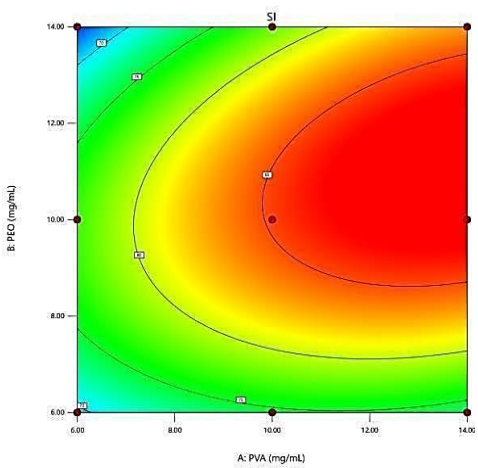

Figure 3: Counterplot of drug loading

Table 9: Thickness of *Boerhavia diffusa* extract loaded Nanofibrous dressing

Formulation	Thickness	Folding endurance	% moisture absorption	% moisture loss	Weight (mg)	Tensile strength (Kg/cm^2)	Drug content (%)
B1	0.069±1.20	302	3.9	3.2	23.45±0.14	2.15	90.15±1.56
B2	0.072±1.45	304	4.1	3.9	25.14±1.04	2.56	91.78±1.47
B3	0.073±1.30	310	3.8	2.7	27.48±1.23	2.14	92.11±1.56
B4	0.074±1.80	308	4.6	4.7	28.04±1.47	2.85	91.98±1.78

application. Swelling index of electrospun nanofibers was measured by a gravimetric technique, influencing drug loading and release. The figure 3 displays swelling degree of drug-loaded nanofiber gels (BDRNF1-BDRNF9) in PBS (pH 7.4) at different intervals: 65.14, 72.08, 75.55, 85.23, 77.91, 83.62, 86.6, 69.86, and 78.82 over 1 to 12 hours (Table 7).

ANOVA for Quadratic Model Response 2: SI

Type III—Partial sum of squares—codes factors. Model F-value 11.88 shows significance, with 3.43% noise chance. Model terms A and B^2 ($p < 0.0500$) are significant, while ones with $p > 0.1000$ are not. The Predicted R^2 (0.4623) is not close to the Adjusted R^2 (0.8718), suggesting potential model or data issues like block effects, outliers, or the need for model reduction. Adeq Precision, with a ratio of 9.888, indicates a sufficient signal for design space navigation.

$SI = 85.21+5.25A+1.68B+3.20AB-2.95A^2-9.07B^2$

Table 10: *In-vitro* diffusion data

Time in hr	% cumulative drug release			
	B1	B2	B3	B4
1	11.45	12.45	17.45	16.23
2	26.89	31.26	30.14	29.87
3	47.48	50.12	47.89	49.55
4	67.59	62.45	69.56	67.44
5	72.65	74.59	74.22	75.45
6	80.45	81.15	82.12	82.97

The coded equation predicts responses using factor levels (+1 for high, -1 for low) and helps compare factor impacts through coefficients. The actual factors equation predicts responses using original units but isn't suitable for comparing factor impacts due to scaled coefficients and a non-centered intercept (Table 8).

Scanning Electron Microscope (SEM)

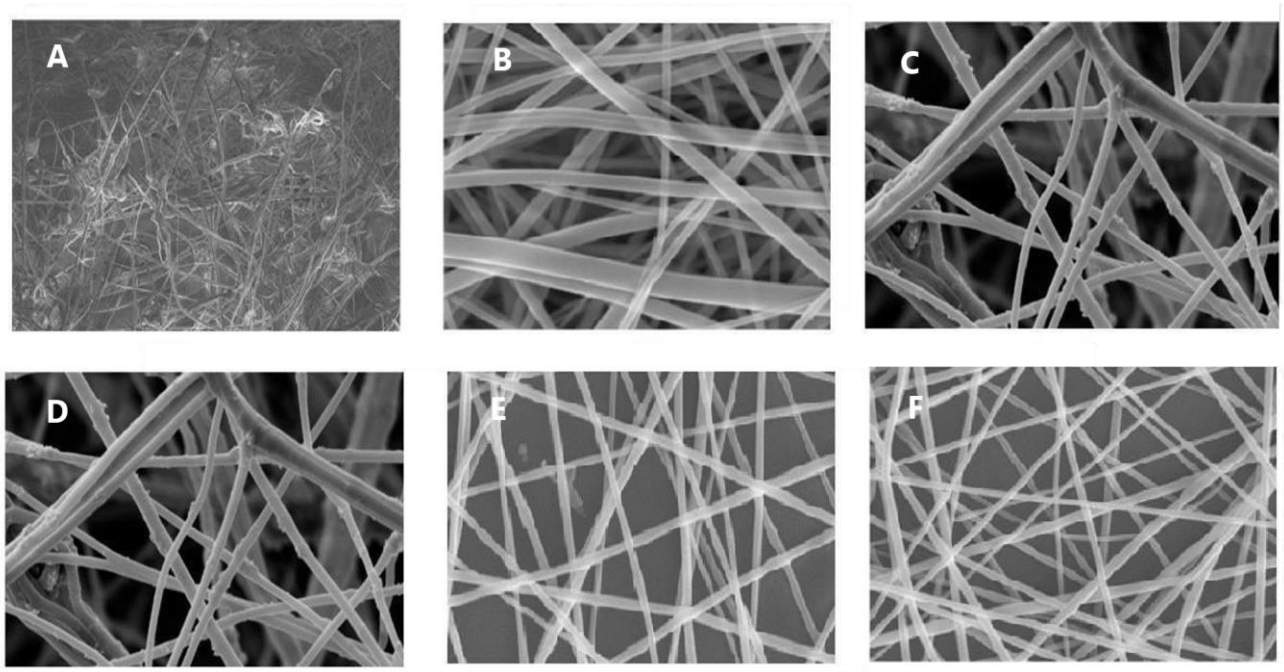

Figure 4: SEM of A- (BDRNF1), B- (BDRNF2),C-(BDRNF3),D-(BDRNF4), E-(BDRNF5), F- (BDRNF6)

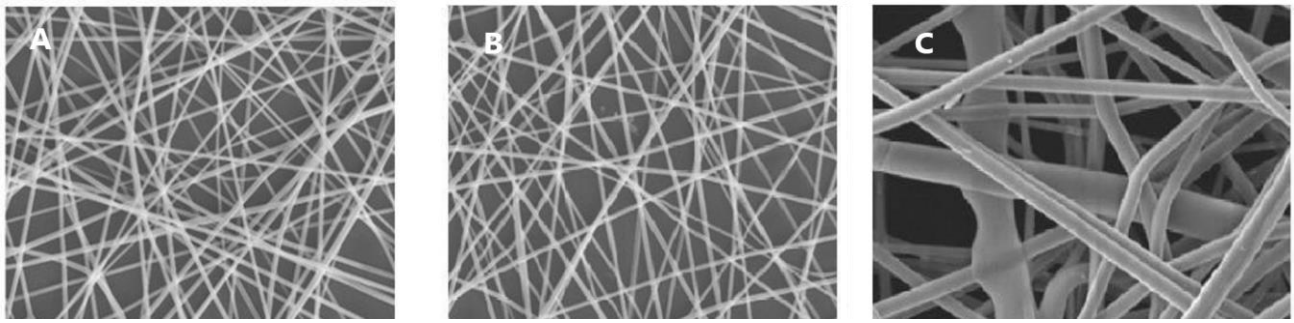

Figure 5: SEM of A-(BDRNF7), B-(BDRNF8), C- (BDRNF9)

Table 11: Wound-healing effect of *Boerhavia diffusa* extract loaded Nanofibrous dressing

Parameter	Wound area (mm^2) & percentage of wound contraction				
Post-wounding Days	Control	B1	B2	B3	B4
Day 0	440.66 ± 2.6757	440 ± 2.1581	440.66 ± 2.1689	503 ± 3.2151	505.66 ± 2.1554
Day 2	428.26 ± 3.1528 (4.24%)	432.66 ± 1.202 (5.47%)	435.33 ± 1.3855* (7.35%)	469.66 ± 1.202 (6.62%)	465.33 ± 1.3335* (7.97%)
Day 4	468.33 ± 1.3336 (15.55%)	324.33 ± 0.589** (21.80%)	384.1 ± 2.714** (27.61%)	393.33 ± 0.989** (21.80%)	366 ± 2.7814** (27.61%)
Day 8	324 ± 1.1549 (32.89%)	285.66 ± 1.545** (40.81%)	289.66 ± 1.641** (42.86%)	292.66 ± 1.3335** (41.81%)	268.66 ± 1.7641** (46.86%)
Day 12	204.66 ± 1.162 (52.47%)	156 ± 1.478** (62.19%)	125 ± 1.218** (71.27%)	165 ± 1.5278** (67.19%)	125 ± 1.3418** (75.27%)
Day 16	77.33 ± 1.4691 (84.64%)	38 ± 1.1549** (95.62%)	17.38 ± 1.202** (97.29)	22 ± 1.1549** (95.62%)	13.66 ± 1.202** (97.29)
Day 18	24.33 ± 1.202 (95.16%)	5.28 ± 0.9546** (98.87%)	00 ± 00** (100%)	5.66 ± 0.9546** (98.87%)	00 ± 00** (100%)
Day 20	9 ± 0.5465 (93.21%)	00 ± 00** (100%)	00 ± 00** (100%)	00 ± 00** (100%)	00 ± 00** (100%)
Period of epithelialization (day)	25.5 ± 0.7416	18.33 ± 0.3058**	17.16 ± 0.7846**	18.33 ± 0.2108**	17.16 ± 0.1666**

n=6,mean±SEM;*P<0.01;**P<0.001

Table 12: Wound-healing effect of *Boerhavia diffusa* extract loaded Nanofibrous dressing

Parameter	Control	B1	B2	B3	B4
Skin breaking strength	275.5 ± 2.2274	266.66 ± 2.5344*	296.66 ± 2.459*	447.66 ± 2.7044*	466.66 ± 2.459*

Silver nanofiber surface morphology was investigated with a Hitachi S-4700 SEM (Hitachi, Japan). For analysis, samples were vacuum-coated with gold sputter and mounted on metal stubs with double-sided adhesive tape (Figure 4, Figure 5).

Characterization of Optimized Batch

FTIR

The functional group's vibrational frequency (cm−1) is 3306.14 for O-H stretch, 1628.82 for C=O stretch, 1457.67 for alkene, and 1076.85 for esters (Figure 6).

XRD

X-ray diffraction (XRD) provides structural information on crystalline compounds. The spectra of the optimized batch (BDRNF7) showed intense peaks, indicating a crystalline structure (Figure 7).

DSC

The DSC spectrum of prepared nanofiber batch BDRNF7 prepared nanofiber batch BDRNF7 showing end set of 133.42°C, which is quite excess when compared with the end set temperature of crude powder melting point of

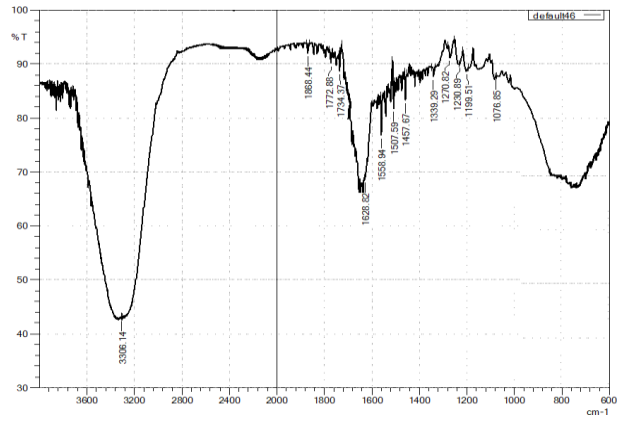

Figure 6: IR spectrum of prepared nanofiber batch BDRNF7

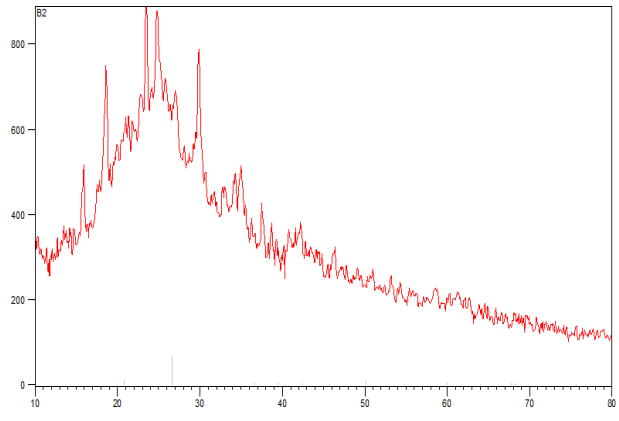

Figure 7: XRD spectrum of prepared nanofiber batch BDRNF7

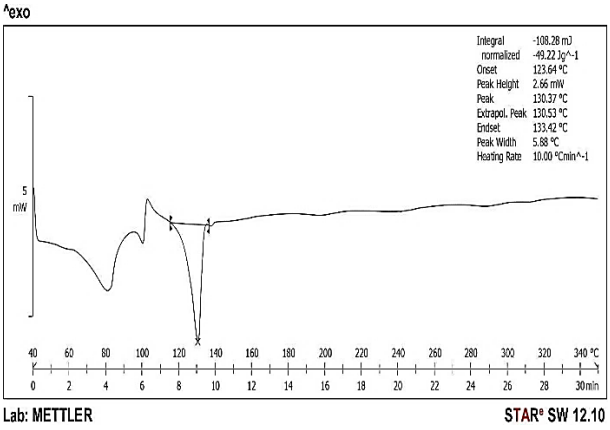

Figure 8: DSC spectrum of prepared nanofiber batch BDRNF7

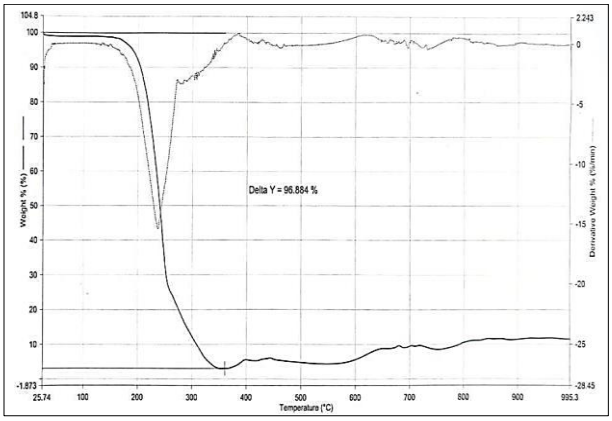

Figure 9: TGA spectrum of prepared nanofiber batch BDRNF7

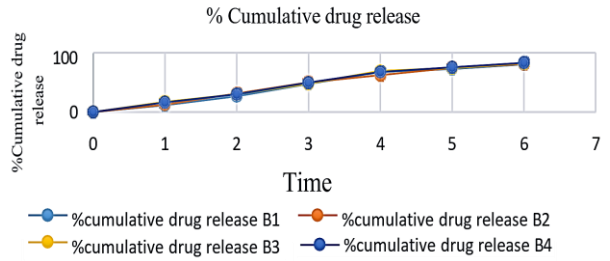

Figure 10: Percent Cumulative drug release for control & Wound Dressing

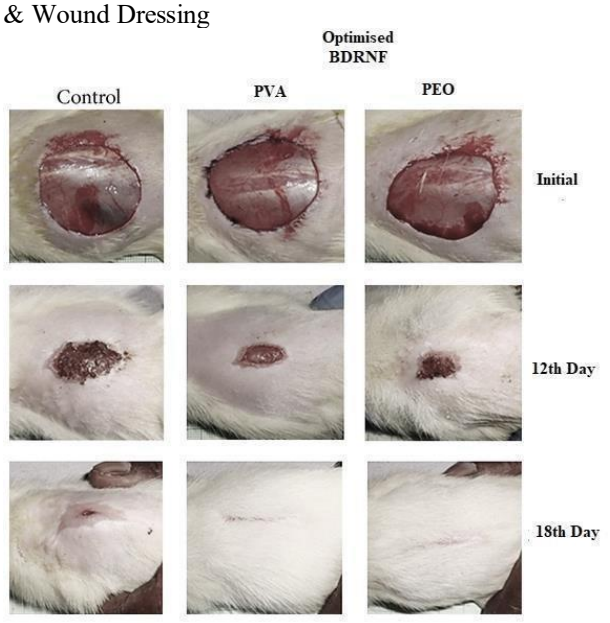

Figure 11: Wound-healing effect of *Boerhavia diffusa* extract loaded Nanofibrous dressing

Boerhavia diffusa (Figure 8).

TGA

TGA thermograms of the prepared nanofiber batch BDRNF7show that the nanofiber gradually decomposed at a higher temperature range (Figure 9).

Characterization of Wound Dressings

The thickness of films B1 and B4 ranged from 0.069 to 0.074, with low standard deviations indicating uniformity. All films showed good folding endurance, ensuring flexibility. Moisture absorption over 3 days varied between 3.8% to 4.6%, while moisture loss ranged from 3.2% to 4.7%. No significant variation in average weight was noted. Tensile strength was between 2.14-2.85 kg/cm², and drug content ranged from 90.15% to 92.11%, demonstrating uniformity (Table 9).

In Vitro Drug Release

The data is demonstrated in (Table 10, Figure 10).

Wound Healing Activity

The effect of wound healing is given in Table 11, Table 12 and Figure 11.

CONCLUSION

In this study, a novel nanofiber patch loaded with *Boerhavia diffusa* root extract was successfully developed and optimized using Response Surface Methodology (RSM) to enhance wound healing. The methanolic extract of *Boerhavia diffusa* was effectively incorporated into a polyvinyl alcohol (PVA) and polyethylene oxide (PEO) matrix, resulting in nanofiber mats with desirable properties. The 3^2 factorial design enabled the systematic optimization of key parameters, leading to the selection of the BDRNF7 batch with 85.12% drug entrapment efficiency and consistent morphology. Furthermore, *in vitro* release studies demonstrated a sustained drug release profile, contributing to prolonged therapeutic effects. Complementary chitosan/alginate membrane dressings were developed to provide additional wound care benefits. In vivo wound healing assessments in animal models revealed that BDRNF7 significantly accelerated wound contraction, enhanced skin breaking strength, and promoted tissue regeneration compared to controls. Moisture interaction studies highlighted the patch's stability under varying humidity, further supporting its suitability for wound management applications. The statistical analysis validated the robustness of the experimental design, with an F-value of 11.88 and an Adjusted R^2 of 0.8718, indicating a strong correlation between experimental and predicted values. Overall, *Boerhavia diffusa*-loaded nanofiber patch demonstrated promising potential as a bioactive wound dressing, offering sustained drug delivery and accelerated wound healing. Future clinical studies are recommended to further evaluate its efficacy and safety in human subjects, paving the way for its application in advanced wound care management.

REFERENCES

1. Malabadi RB, Kolkar KP, Acharya MB, Nityasree BR, Chalannavar RK. Wound healing: role of traditional herbal medicine treatment. International Journal of Innovation Scientific Research and Review. 2022;4(6):2856-74.
2. Agarwal S, Wendorff JH, Greiner A. Use of electrospinning technique for biomedical applications. Polymer. 2008 Dec 8;49(26):5603-21.
3. Sen CK. Human wounds and its burden: an updated compendium of estimates. Advances in wound care. 2019 Feb 1;8(2):39-48.
4. Monika P, Waiker PV, Chandraprabha MN, Rangarajan A, Murthy KN. Myofibroblast progeny in wound biology and wound healing studies. Wound Repair and Regeneration. 2021 Jul;29(4):531-47.
5. Gonzalez AC, Costa TF, Andrade ZD, Medrado AR. Wound healing-A literature review. Anais brasileiros de dermatologia. 2016;91(5):614-20.
6. Ghodela NK, Dudhamal T. Wound healing potential of Ayurved herbal and herbo-mineral formulations: A brief review. International Journal of Herbal Medicine. 2017;5(1):39-45.
7. Han G, Ceilley R. Chronic wound healing: a review of current management and treatments. Advances in therapy. 2017 Mar;34:599-610.
8. Xie B, Lu S, Wang L, Zhou Z, Wang W, Lou C, Zhang Y, Yuan Z, Liu H, Cui L, Qiu J. Intra or extracellular: The location of piezotronic effect determines the polarization regulation of macrophages for enhanced wound healing. Nano Energy. 2025 Jun 1;138:110893.
9. Mi Y, Yang F, Bloomquist C, Xia Y, Sun B, Qi Y, Wagner K, Montgomery SA, Zhang T, Wang AZ. Biologically targeted photo-crosslinkable nanopatch to prevent postsurgical peritoneal adhesion. Advanced Science. 2019 Oct;6(19):1900809.
10. Mishra S, Aeri V, Gaur PK, Jachak SM. Phytochemical, therapeutic, and ethnopharmacological overview for a traditionally important herb: *Boerhavia diffusa* Linn. BioMed research international. 2014;2014(1):808302.
11. Rawat AK, Mehrotra S, Tripathi SC, Shome U. Hepatoprotective activity of Boerhaavia diffusa L. roots—a popular Indian ethnomedicine. Journal of ethnopharmacology. 1997 Mar 1;56(1):61-6.
12. Bhardwaj N, Kundu SC. Electrospinning: A fascinating fiber fabrication technique. Biotechnology advances. 2010 May 1;28(3):325-47.
13. Thakkar S, Misra M. Electrospun polymeric nanofibers: New horizons in drugdelivery. European Journal of Pharmaceutical Sciences. 2017 Sep 30;107:148-67.
14. Aggarwal A, Sharma L, Sharma D, Dhobale S, Deshmukh N, Barde L, Tare H. Nutritional Significance of Benincasa hispida. International Journal of Pharmaceutical Quality Assurance. 2023;14(2):410-415.
15. Anjum S, Gupta A, Sharma D, Gautam D, Bhan S, Sharma A, Kapil A, Gupta B. Developmentof novel wound care systems based on nanosilvernanohydrogels of polymethacrylic acid with Aloe vera and curcumin. Materials Science and Engineering: C. 2016 Jul 1;64:157-66.
16. Joshi S, Sharma L, Tare M, Baheti D, Dama G, Tare H. The Nutritional Needs of Mothers and Babies: A Review. International Journal of Pharmaceutical Quality Assurance. 2023;14(2):421-425.
17. Eatemadi A, Daraee H, Zarghami N, MelatYar H, Akbarzadeh A. Nanofiber: Synthesis and biomedical applications. Artificial cells, nanomedicine, and biotechnology. 2016 Jan 2; 44(1):111-21.
18. Arora A, Sharma L, Sharma D, Ghangale G, Bidkar J, Tare H. The Nutraceutical Role of Pumpkin Seed and its Health Effect: A Review. International Journal of Pharmaceutical Quality Assurance. 2023;14(1):233-238.
19. Noothi S, Malothu N, Desu PK, Kumar S. Implication of Central Composite Design in the Development of Simvastatin-Loaded Nanosponges. International Journal of Applied Pharmaceutics. 2023;15(5):227-36.
20. Arthanari S, Mani G, Jang JH, Choi JO, Cho YH, Lee JH, Cha SE, Oh HS, Kwon DH, Jang HT. Preparation and characterization of gatifloxacin-loaded alginate/poly (vinyl alcohol) electrospun nanofibers. Artificial cells, nanomedicine, and biotechnology. 2016 Apr 2;44(3):847-52.
21. Dhobale G, Dhobale S, Hande R, Tare H. Formulation and Ev aluation of Brucine Sulphate Transdermal Patch for Anti-Inflammatory Activity. International Journal of Drug Delivery Technology. 2024;14(2):945-947
22. Hajare P, Rai V, Nipate S, Balap A, Pimple B, Chumbhale D, Gaikwad A, Tare H. Anti-arthritic potential of ethyl acetate fraction of Pinus roxburghii Sargent stem bark in Freund's complete adjuvant induced arthritis in Wistar rats. Multidisciplinary Science Journal. 2023 Jun 7;5(4):2023046-.
23. Pawar S, Shende P, Trotta F. Diversity of β-cyclodextrin-based nanosponges for transformation of actives. International Journal of Pharmaceutics. 2019 Jun 30;565:333-50.
24. Moin A, Roohi NF, RizviSM, Ashraf SA, SiddiquiAJ, Patel M, Ahmed SM, Gowda DV, Adnan M. Design and formulation of polymeric nanosponge tablets with enhanced solubility for combination therapy. RSC advances. 2020;10(57):34869-84.
25. Yang W, He X, Luzi F, Dong W, Zheng T, Kenny JM, Puglia D, Ma P. Thermomechanical, antioxidant and moisture behaviour of PVA films in presence of citric acid esterified cellulose nanocrystals. International Journal of Biological Macromolecules. 2020 Oct 15;161:617-26.